



Immobilization of Superoxide Dismutase in Mesoporous Silica and its Applications in Strengthening the Lifespan and Healthspan of *Caenorhabditis elegans*

Yiling Yang^{1*}, Wenbin Wang², Kefeng Liu² and Jie Zhao^{2,3*}

¹Department of Ultrasound, The First Affiliated Hospital of Zhengzhou University, Zhengzhou, China, ²Department of Pharmacy, The First Affiliated Hospital of Zhengzhou University, Zhengzhou, China, ³Internet Medical and System Applications of National Engineering Laboratory, Zhengzhou, China

OPEN ACCESS

Edited by:

Wooram Park,
Sungkyunkwan University, South
Korea

Reviewed by:

Jianbo Jia,
Guangzhou University, China
Eunsoo Yoo,
North Carolina Agricultural and
Technical State University,
United States

*Correspondence:

Yiling Yang
fccyangyl@zzu.edu.cn
Jie Zhao
zhaojiezzu@163.com

Specialty section:

This article was submitted to
Nanobiotechnology,
a section of the journal
Frontiers in Bioengineering and
Biotechnology

Received: 15 October 2021

Accepted: 11 May 2022

Published: 19 July 2022

Citation:

Yang Y, Wang W, Liu K and Zhao J
(2022) Immobilization of Superoxide
Dismutase in Mesoporous Silica and its
Applications in Strengthening the
Lifespan and Healthspan of
Caenorhabditis elegans.
Front. Bioeng. Biotechnol. 10:795620.
doi: 10.3389/fbioe.2022.795620

Senescence is a major inductive factor of aging-related diseases in connection with an accumulation of reactive oxygen species (ROS). Therefore, it is important to maintain ROS at an appropriate level to keep homeostasis in organisms. Superoxide dismutase (SOD) is a vital enzyme in defending against oxidative damage *in vivo*. Because of the defects in the direct application of SOD and SOD mimics, mounting delivery systems have been developed for the efficient applications of SOD to realize antioxidant treatment. Among these systems, mesoporous silica nanoparticles (MSNs) have been widely studied because of various advantages such as desirable stability, low toxicity, and adjustable particle sizes. Herein, SOD was immobilized on MSNs using a physical absorption strategy to construct the nanosystem SOD@MSN. The nematode *Caenorhabditis elegans* (*C. elegans*) was selected as the model organism for the subsequent antioxidant and anti-aging studies. The research results suggested the nanosystem could not only be effectively internalized by *C. elegans* but could also protect the nematode against external stress, thus extending the lifespan and healthspan of *C. elegans*. Therefore, SOD@MSN could be applied as a promising medicine in anti-aging therapeutics.

Keywords: ROS, SOD@MSN, *C. elegans*, lifespan, healthspan, anti-aging therapeutics

INTRODUCTION

Senescence, which enhances susceptibility to stimulation and increases the rate of death, is a gradual physiological deterioration with age. The biological mechanism of aging is still unknown (Wurm et al., 2020; Portegijs et al., 2022). Nowadays, a number of research studies have found that reactive oxygen species (ROS) have a close relationship with aging and homeostasis in organisms (Qi et al., 2019; Yang et al., 2019). ROS, which is frequently mentioned in the field of biology and medicine, refers to oxygen-containing substances with high reactivity, specifically superoxide anion (O_2^-), hydrogen peroxide (H_2O_2), hydroxyl radical (OH), singlet oxygen (1O_2), peroxide free radical (LOO), hydrogen peroxide lipid (LOOH), peroxy nitro group ($ONOO^-$), hypochlorous acid (HOCl), and ozone (O_3) (Liu T. et al., 2020; Gao et al., 2021). Although ROS generated in the process of oxygen metabolism are essential for cell signaling and immune response, superfluous ROS could oxidize lipids, proteins, and nucleic acid, thus triggering various diseases such as inflammation, stroke,

cancer, Alzheimer's disease, and Parkinson's disease (Zhao et al., 2019; Liu Y. et al., 2020; Ma et al., 2020; Yu et al., 2020). More critically, the accumulation of ROS could reduce the resistance against cellular stress including thermal and oxidative stimulation, thus accelerating the process of aging (Shi et al., 2018). Current studies aim to design drugs to improve the physiological conditions and inhibit the degeneration of age-related diseases by eliminating ROS (Wang Z. et al., 2017). *Caenorhabditis elegans* (*C. elegans*), as a kind of pseudo-coelomate nematode, has been widely applied as a model organism for aging research due to its behavioral and physiological similarity with humans when they age (Zhang et al., 2016). Notably, similar to various species, *C. elegans* accumulate oxidized proteins and have autofluorescence as they age (Meyer et al., 2010; Yee et al., 2014).

To fight against damage by ROS and maintain the oxidation level at the appropriate level, it is critical to find a well-performing antioxidant. Nowadays, various antioxidants including synthetic antioxidants, polysaccharides, and proteinaceous antioxidants have been adopted in the removal of ROS production to delay aging (Owusu-Ansah et al., 2013; Xia et al., 2013). Compared with synthetic antioxidants or polysaccharide, proteinaceous antioxidants including superoxide dismutase (SOD), catalase (CAT), and glutathione peroxidase (GPx) are more acceptable due to their excellent biocompatibility and better ability to scavenge free radicals (Wang et al., 2020; Huang et al., 2021). Previous investigators have examined the effects of overexpression of CAT genes targeting mitochondria that confer resistance to oxidation on extending the lifespan of mice. Meanwhile, results showed that reducing the mitochondrial ROS level might be important in determining mammalian longevity (Qin et al., 2020; Xi et al., 2020; Zhang et al., 2021).

SOD, as an important member of the antioxidative system, can efficiently catalyze the decomposition of superoxide radicals into hydrogen peroxide and oxygen (Udipi et al., 2000; Singh et al., 2017; Koner et al., 2021; Liu et al., 2021; Wu et al., 2021). Therefore, it has demonstrated therapeutic potential in the treatment of ROS-mediated diseases and aging. However, direct use of SOD has been hampered by poor pharmacokinetics, rapid renal clearance, degradation by proteases in the serum, and low cellular membrane-penetrating ability (Darroudi et al., 2020; Rao et al., 2021). Thus, it is necessary to develop several techniques to enhance the stability and cellular delivery ability of SOD, such as PEGylation or encapsulating proteins in vesicles (Xu et al., 2021), liposomes (Abedi Gaballu et al., 2019; Li et al., 2020), and mesoporous silica nanoparticles (MSN) (von Baeckmann et al., 2018; Wang et al., 2019). Among them, MSNs, as a kind of safe medical material approved by the United States Food and Drug Administration (FDA), have been extensively studied and applied in drug delivery due to their high specific surface area, stable pore volume, adjustable particle size, and excellent biocompatibility (Wang et al., 2016; Wen et al., 2017). In addition, the particle sizes of MSNs can be designed to be less than 100 nm, which have a larger specific surface area and are more suitable for biomedical applications (Zhang et al., 2018).

In this study, an assembly enzyme SOD@MSN was constructed by physical absorption, and the antioxidant effects

of SOD@MSN were investigated. In addition, we revealed the protective effect of this assembly enzyme against stress and the anti-decrepit and life-prolonging effect of SOD@MSN on *C. elegans*. The relationship among these effects is also discussed. The mechanism of action is also expounded, including the assembly's antioxidant activity and the effects on stress-related proteins and genes.

MATERIALS AND METHODS

Materials

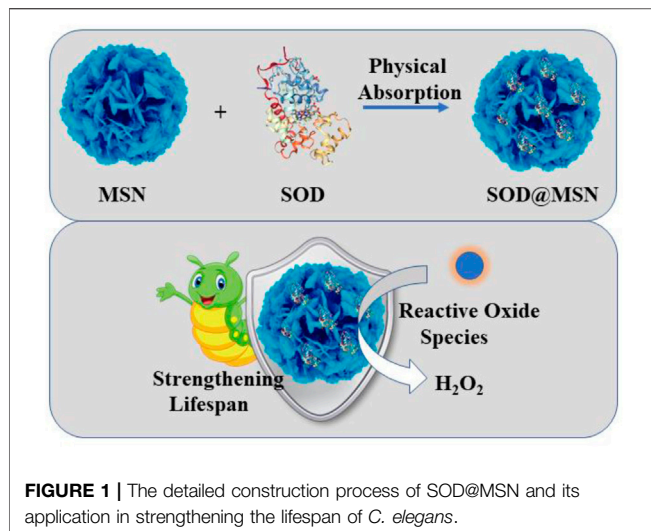
Cetyltrimethylammonium bromide (CTAB), tetraethyl orthosilicate (TEOS), 1,2-Bis(triethoxysilyl) ethane (BTEE), triethanolamine (TEA), and sodium salicylate (NaSal) were purchased from Sigma-Aldrich. Hydrochloric acid (HCl), ethanol, and methanol were purchased from Aladdin. In addition, 5-fluoro-2-deoxyuracil (FUDR) and phenylmethyl sulfonyl chloride (PMSF) were purchased from Sigma Corporation (United States); SOD enzyme was purchased from Bairdi Company (Beijing, China). TRNzol Universal Reagent was purchased from TIANGEN (Beijing, China); PrimeScript™ RT kit and SYBR® Premix Ex Taq™ kit were purchased from TAKARA Company (Dalian, China). All chemicals were used as received without purification.

Synthesis of Mesoporous Silica Nanoparticles and Superoxide Dismutase@ Mesoporous Silica Nanoparticles

MSN and SOD@MSN were achieved through a one-pot synthesis using the cationic surfactant CTAB, NaSal as the structure-directing agent, TEOS and BTEE as silica sources, and TEA as a catalyst. A typical synthesis of MSN was carried out as follows: First, 0.05 g TEA was dissolved in 15 ml of water and stirred gently at 80°C in an oil bath under a magnetic stirring for 1 h. Then, 360 mg CTAB and 150 mg NaSal were added to the aforementioned solution and then stirring was continued for another 1 h. A mixture of 1.8 ml TEOS and 1.5 ml BTEE was added to the NaSal-TEA solution with or without SOD with gentle stirring for 10 h. The products were collected by centrifugation and washed five times with ethanol. Then, the obtained products were extracted with HCl and methanol solution at 60°C for 5 h to eliminate the template, and then dried in a vacuum at room temperature for 12 h.

Synthesis of FITC-Superoxide Dismutase@ Mesoporous Silica Nanoparticles

20 mg SOD and 10 mg FITC were dissolved in 50 ml phosphate buffer (50 mM, pH 8.0), and the mixture was stirred at 180 rpm at room temperature for 24 h. The sample was then washed with distilled water using Amicon® ultra-15 until no absorption value could be detected in the ultrafiltration supernatant at 488 nm. Finally, FITC-SOD was obtained by freeze-drying and used as raw material. The synthetic method of FITC-SOD@MSN was the same as the aforementioned method.



Determination of the Relative Enzymatic Activity

The load of lipase in SOD@MSN was calculated by formula $A - A_1 / B \times 100\%$, where A, A_1 , and B, respectively, represent the weight of input SOD, the weight of SOD in the supernatant after reaction, and the total weight of SOD@MSN synthesized. The quality of lipase in the supernatant was determined by the BCA protein quantification kit (Beyotime, Nanjing, China). The enzymatic activity was assessed by the pyrogallol autoxidation assay. In detail, 240 μ l enzyme solutions (1 mg/ml) was added to 750 μ l Tris-HCL (pH 8.2) and incubated for 20 min. 10 μ l pyrogallol solution (50 mM) was then mixed into the enzyme solutions and the absorbance at 325 nm was measured for 1 min by the UV-2700 spectrometer (Shimadzu, Kyoto, Japan).

Worm Strains and Culture

C. elegans was cultured in a nematode growth medium (NGM) covered with *E. coli* OP50 at 20°C. To obtain a synchronous nematode, we cultured gravid worms for 5 h and then the eggs were collected by treating the eggs and adult *C. elegans* with alkaline hypochlorite solution (NaOH: NaClO: H₂O = 2:1:1); we continued to culture in the NGM medium for about 12 h. The worms of the control group were cultured in NGM plates coated

with 5-fluoro-20-deoxyuridine (FUDR, 100 μ M) dissolved in *E. coli* OP50, and FUDR was used to prevent progeny growth. The worms in the treatment groups were grown in NGM medium coated with SOD@MSN, free SOD or MSN, and FUDR dissolved in *E. coli* OP50.

Uptake of Superoxide Dismutase@ Mesoporous Silica Nanoparticles by *C. elegans*

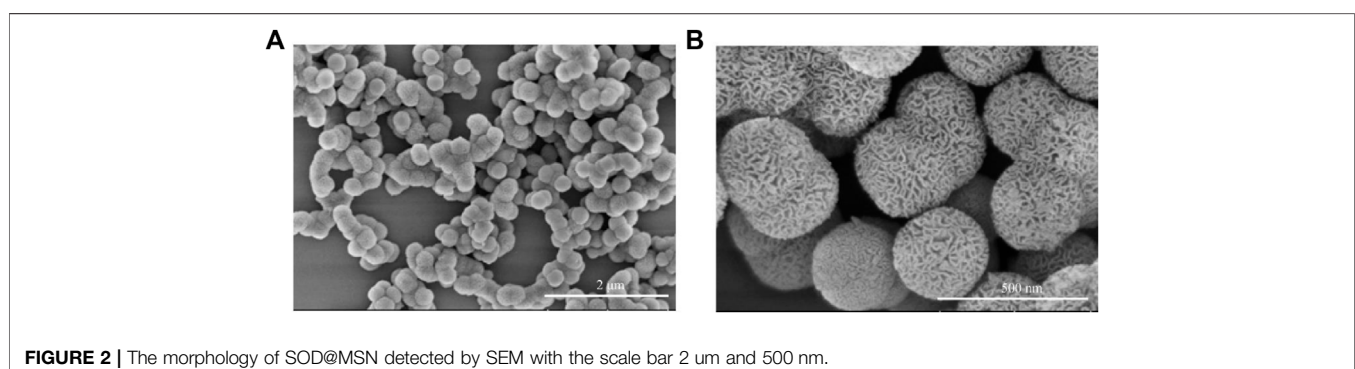
In order to observe the effect of SOD and SOD@MSN uptake by nematodes more intuitively, we labeled SOD with FITC, and then assembled FITC-SOD onto MSN. The L4-stage nematodes were transferred to NGM culture plates containing FITC-SOD, FITC-SOD@MSN, or MSN for 2 h. The nematodes were then washed from the NGM culture plate with M9 buffer and centrifuged (2000 rpm, 1 min) for collection. Then, the nematodes were anesthetized with levamisole and transferred to slides containing 3% agarose for fixation. Finally, the nematodes were observed and photographed under a fluorescence microscope.

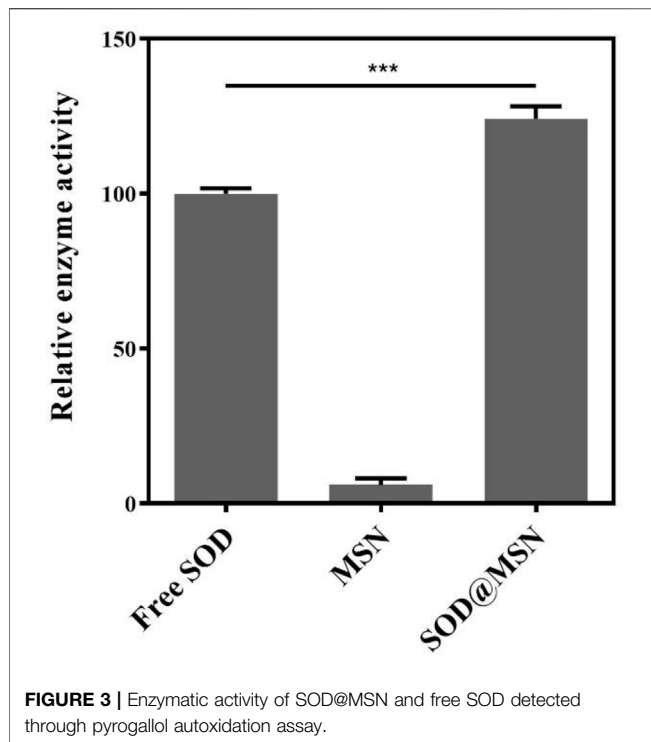
In vivo Retention Time of Superoxide Dismutase@Mesoporous Silica Nanoparticles in *C. elegans*

C. elegans at the L4 stage were cultured in NGM culture plates containing FITC-SOD or FITC-SOD@MSN for 6 h and then transferred to fresh NGM culture plates for further culture. At 0.5, 1, 2, 4, 6, 8, 10, 12, 14, 16, and 18 h, three nematodes were removed from the two groups of culture plates, respectively. After levamisole anesthesia, the nematodes were fixed to a glass slide containing 3% agarose. Fluorescence microscopy was used to observe the changes of FITC fluorescence in nematodes at different times, and photographs were taken until the fluorescence in nematodes of the FITC-SOD group was completely quenched. The fluorescence intensity *in vivo* was quantified by ImageJ software.

Lifespan Assay

C. elegans was used in the lifespan assay at least three times independently at 20°C. The assay started when the synchronous worms were grown to the end stage of Level four, which was set as day 1. There were 80 worms in each of the groups, and the fresh





treatment plates were replaced every 2 days. Tested *C. elegans* were considered to be dead when they failed to respond under the stimulus of a platinum wire.

Healthspan Assay

Oil Red O stain which has been widely regarded as a dye for lipid deposits was used for the detection of the fat levels in *C. elegans*. Forty synchronous worms per group were raised to the L4 level, which was regarded as day 0. Furthermore, the worms were transferred to plates with or without SOD formulations and continued to culture for 5 days. Then, the nematodes of various groups were washed with PBS three times and fixed with 1% paraformaldehyde for 20 min. Subsequently, the *C. elegans* was subjected to three repeated freezing and thawing between -80 and 40°C , after which the worms were treated with 60% isopropanol to dehydration. Finally, 60% Oil-Red-O staining solution was added and stained for 20 min followed by washing with PBS two times and photograph collection by fluorescence microscopy.

The spontaneous fluorescence was then detected as a signal of aging. Fifty animals per group were cultured from L1 level on the NGM plates with or without drugs. After ten days, the worms were washed with M9 buffer three times and anesthetized with levamisole. Afterward, 3% agarose pads were used to immobilize the worms, and then the spontaneous fluorescence was visualized through fluorescence microscopy and quantified by ImageJ. All experiments were performed in triplicate.

Assessment of Stress Resistance

The age-synchronized *C. elegans* were first cultured on NGM plates with or without samples at 20°C for 2 days, and then subjected to plates with juglone ($500\ \mu\text{M}$). The survival worms were recorded every hour over 12 h.

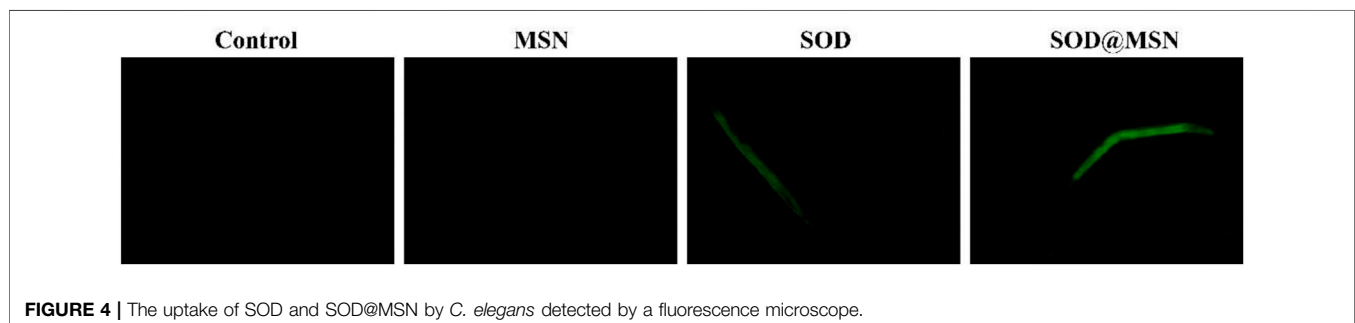
The selected 2-day-old nematodes were subjected to the same treatment as described above for 48 h and then incubated at 35°C , which was considered a thermal stimulation. The number of surviving animals was recorded over 8 h, and all experiments were conducted at least three times.

Assessment of Intracellular Reactive Oxygen Species Levels

The worms that had just grown up into adults were selected for the experiment. For detection under normal conditions, the animals were treated with various SOD formulations for 2 days. For detection under oxidative environment, the worms were first subjected to juglone ($300\ \mu\text{M}$) before treatment with samples for 2 days. Subsequently, the animals were washed and collected by M9 buffer in suspension. Finally, ROS fluorochrome H2DCF-DA and the suspension of worms were pipetted into 96-well plates, respectively, with the final concentration of H2DCF-DA at $50\ \mu\text{M}$. The fluorescence was detected every 30 min over 150 min at 20°C by a microplate fluorescence reader (Olympus, Tokyo, Japan) with excitation/emission wavelengths at 485 and 538 nm, respectively. The fluorescence intensity at 30 min without drugs' treatment was set as 100%.

Assessment of Intracellular Superoxide Dismutase Activity

N2 worms were cultured on NGM plates with or without drugs' treatment for one week. During this process, the worms were transferred to fresh plates every 2 days. Afterward, the total



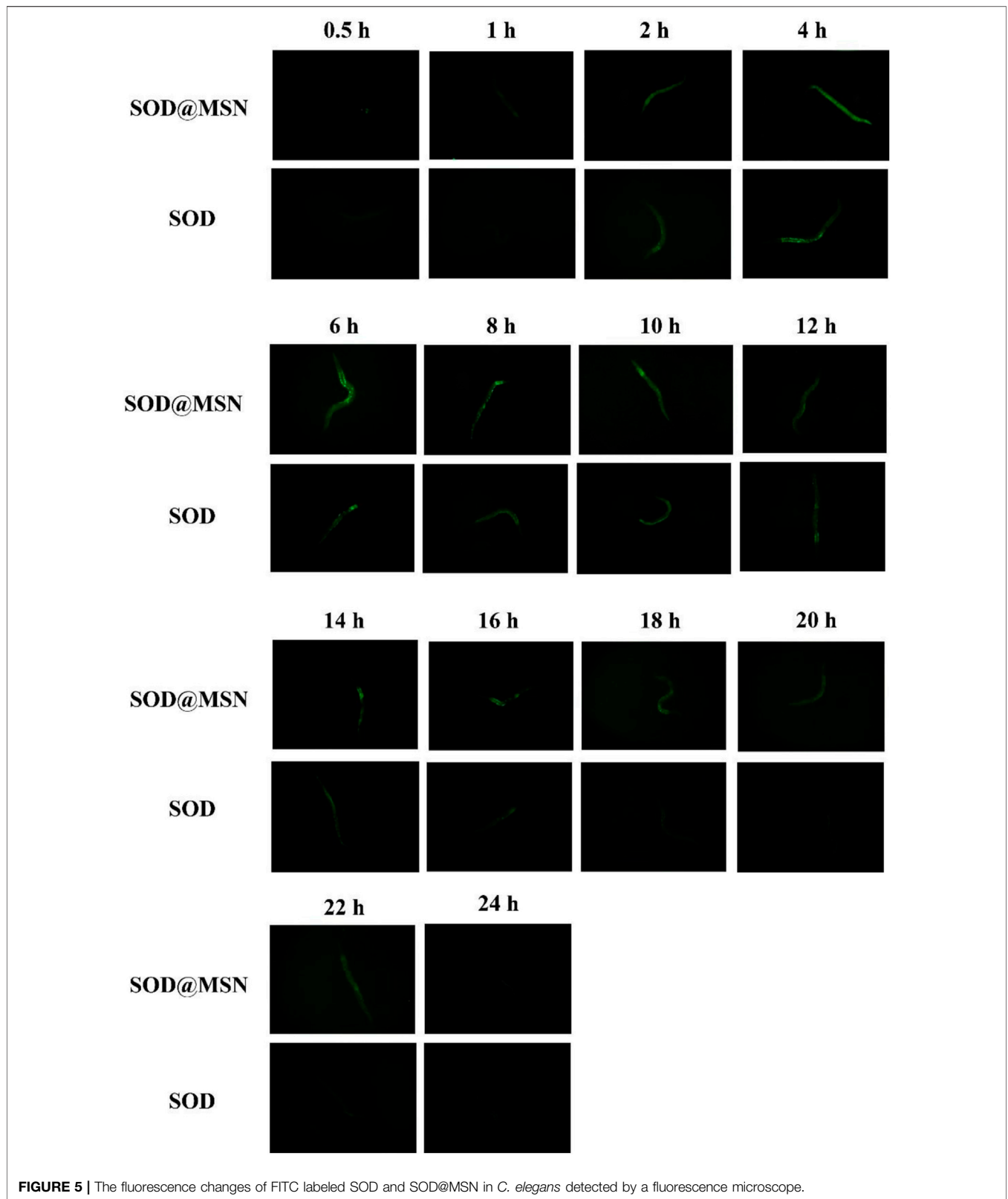


FIGURE 5 | The fluorescence changes of FITC labeled SOD and SOD@MSN in *C. elegans* detected by a fluorescence microscope.

protein in nematodes was extracted. Briefly, the animals were washed down to the EP tubes using M9 buffer and centrifuged at 1,000 rpm for 2 min to remove M9. Subsequently, 150 μ l RIPA

with 1.5 μ l PMSF was added to re-suspend the worms, and then the samples were subjected to three fast freeze–thaw cycles. Finally, the total protein was collected by centrifuging at

8,000 rpm for 1 min, and the supernatants were used to detect the SOD enzymatic activity by Total Superoxide Dismutase Assay Kit with WST-8 (Beyotime). To normalize the enzymatic activity, the protein concentration was measured by BCA assay kit (Beyotime).

Quantitative Real-Time PCR

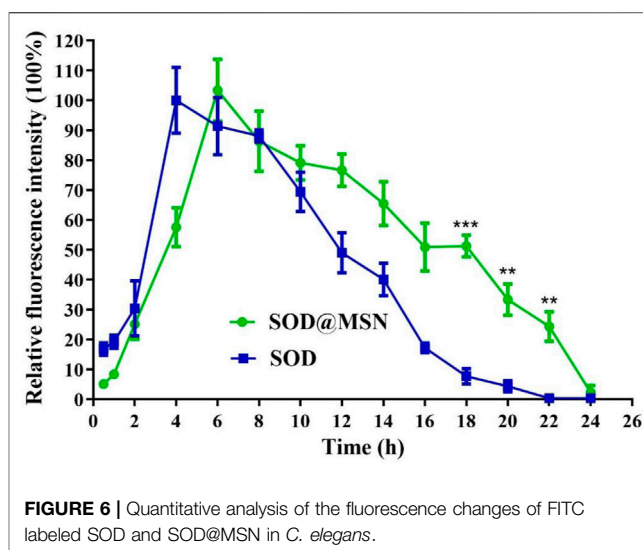
After treatment with or without SOD formulations for 2 days, total RNAs of the worms were extracted with Trizol Reagent, and cDNA was generated by PrimeScript® RT reagent Kit. Afterward, the mRNA expressions of *cdc-42*, *daf-16*, *daf-2*, *sod-3*, *hsp-16.2*, and *skn-1* were determined on a 7500 Real-Time PCR System (Applied Biosystems, Foster City, CA) using SYBR green as the detection reagent. The data were calculated using the $2^{-\Delta\Delta CT}$ method, and *cdc-42* was used as a control gene for normalization. The primers were as follows:

daf-16 forward: 5'-TTTCCGTCCCCGAACTCAA-3';
reverse: 5'-ATTC-GCCAACCCATGATGG-3';
sod-3 forward: 5'-AGCATCATGC-CACCTACGTGA-3';
reverse: 5'-CACCACCATTGAATTCAGCG-3';
daf-2 forward: 5'-GGCCGTAGGACGTTTA-TTTG-3';
reverse: 5'-TTCCACAGTGAAGAAGCCTGG-3';
hsp-16.2 forward: 5'-C-GTCGAAGAGAATACTGCTGAA-3';
reverse: 5'-TGCAGCGAACATAACT-GTATATTTAG-3';
skn-1 forward: 5'-AGTGTCGGCGTTC-CAGATTTC-3';
reverse: 5'-GTCGACGAATCTTGCGAATCA-3';
cdc-42 forward: 5'-CTGCTGGACAGGAAGATTACG-3';
reverse: 5'-CTCGGACATTCTCGA ATGAAG-3'.

RESULTS AND DISCUSSION

Synthesis and Electron Microscopic Analysis of Superoxide Dismutase@ Mesoporous Silica Nanoparticles

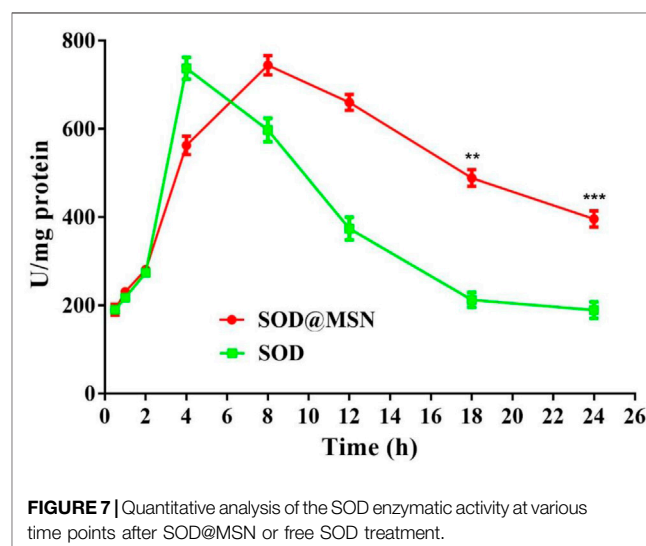
First, we synthesized SOD@MSN with various ligand ratios (TEOS: BTEE from 0.8 to 1.4) and found that only the given ligand ratio and reaction conditions could obtain the homogeneous morphology of SOD@MSN (Figures 1, 2 and Supplementary Figure S1). In addition, SOD content was 10.36 wt% in SOD@MSN determined by BCA quantitative method. SOD@MSN at the given dose possessed the best SOD activity under the same SOD content (Supplementary Figure S2) and the enzymatic activity was concentration-dependent (Supplementary Figure S3). The nanosystem was constructed through physical absorption (Wang P. et al., 2017). The morphology of nanomaterial SOD@MSN was characterized by SEM (Figure 2), which evidently illustrated that SOD@MSN had a regular sphericity and suitable particle size to be intake by *C. elegans*. The zeta potential distribution of SOD@MSN was also determined, which suggested that the surface charge were +35.5 and +39.0 mV in water and PBS solutions, respectively (Supplementary Figure S4). Further, the enzymatic activity

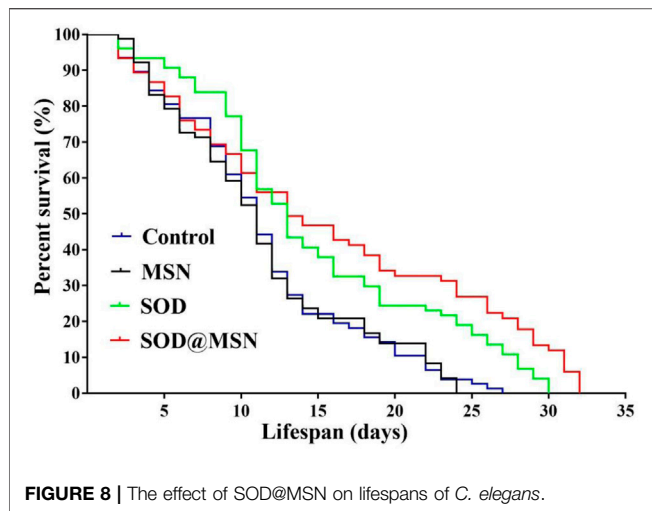


of SOD@MSN was detected by pyrogallol autoxidation assay, which suggested that the SOD activity was significantly increased by assembling into MSN (Figure 3).

Uptake Efficacy of Superoxide Dismutase@ Mesoporous Silica Nanoparticles by *C. elegans* and *in vivo* Stability

Effective entry of assembling enzymes into *C. elegans* is the prerequisite for them to exert an antioxidant role. Therefore, we first studied the uptake capacity of *C. elegans* to SOD@MSN and its stability in worms. The results were shown in Figure 4. Both FITC-SOD@MSN- and FITC-SOD-treated nematodes showed green fluorescence, indicating that SOD@MSN and free SOD could be absorbed by nematodes. Then, *C. elegans*



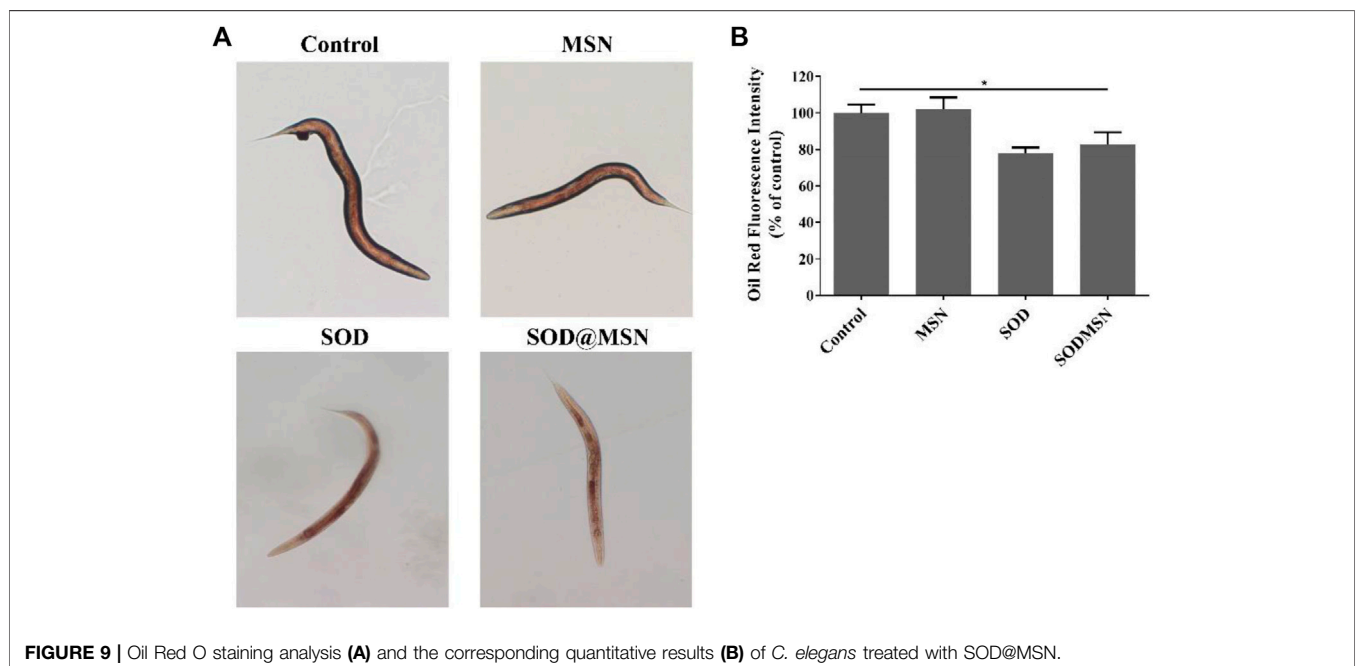


were treated with FITC-labeled free enzymes or assembled enzymes for 6 h, and then transferred to NGM culture plates without fluorescence. The quenching of FITC fluorescence in

nematodes was observed and recorded during the whole culture process, and the degradation rate of FITC in nematodes was investigated. **Figure 5** showed that the fluorescence of nematodes in both FITC-SOD@MSN and FITC-SOD groups underwent a change from weak to strong and then to weak. Fluorescence quantitative results obtained by ImageJ software (**Figure 6**) showed that the fluorescence of *C. elegans* treated with FITC-SOD@MSN reached the maximum at the sixth hour, while that of nematode treated with FITC-SOD reached the maximum at the fourth hour, indicating that the absorption of nematode to SOD@MSN was slightly slower than that of free SOD. However, the fluorescence of FITC-SOD@MSN treated nematodes was still obvious at the eighteenth hour, while the fluorescence of FITC-SOD-treated nematodes was almost completely quenched. At the same time, the fluorescence intensity of the FITC-SOD@MSN-treated group was higher than that of free SOD in the range of 12 to 22 h. In addition, the sizes of SOD@MSN in *C. elegans* were detected in a time-dependent manner, which suggested that the size of the nanoparticle in the body of *C. elegans* remained around 300 nm (**Supplementary Figure S5**). Furthermore, the SOD enzymatic activity detection at various time points after

TABLE 1 | Statistical table of the influence of SOD@MSN on the mean life span, mean life change, and maximum life span of *C. elegans*.

Genotype	Food	Treatment (20°C)	Total (N)	Mean		Maximum lifespan	Change in mean lifespan (%)	Log-rank test	
				Lifespan	SE			χ^2	P
Wild-type	OP50	Control	80	10.23	0.424	26			
Wild-type	OP50	SOD@MSN	75	16.12	1.678	33	36.49	6.214	0.0045
Wild-type	OP50	SOD	75	14.04	0.862	31	25.83	3.456	0.0483
Wild-type	OP50	MSN	80	9.78	0.810	23	-3.42	0.0382	0.8016



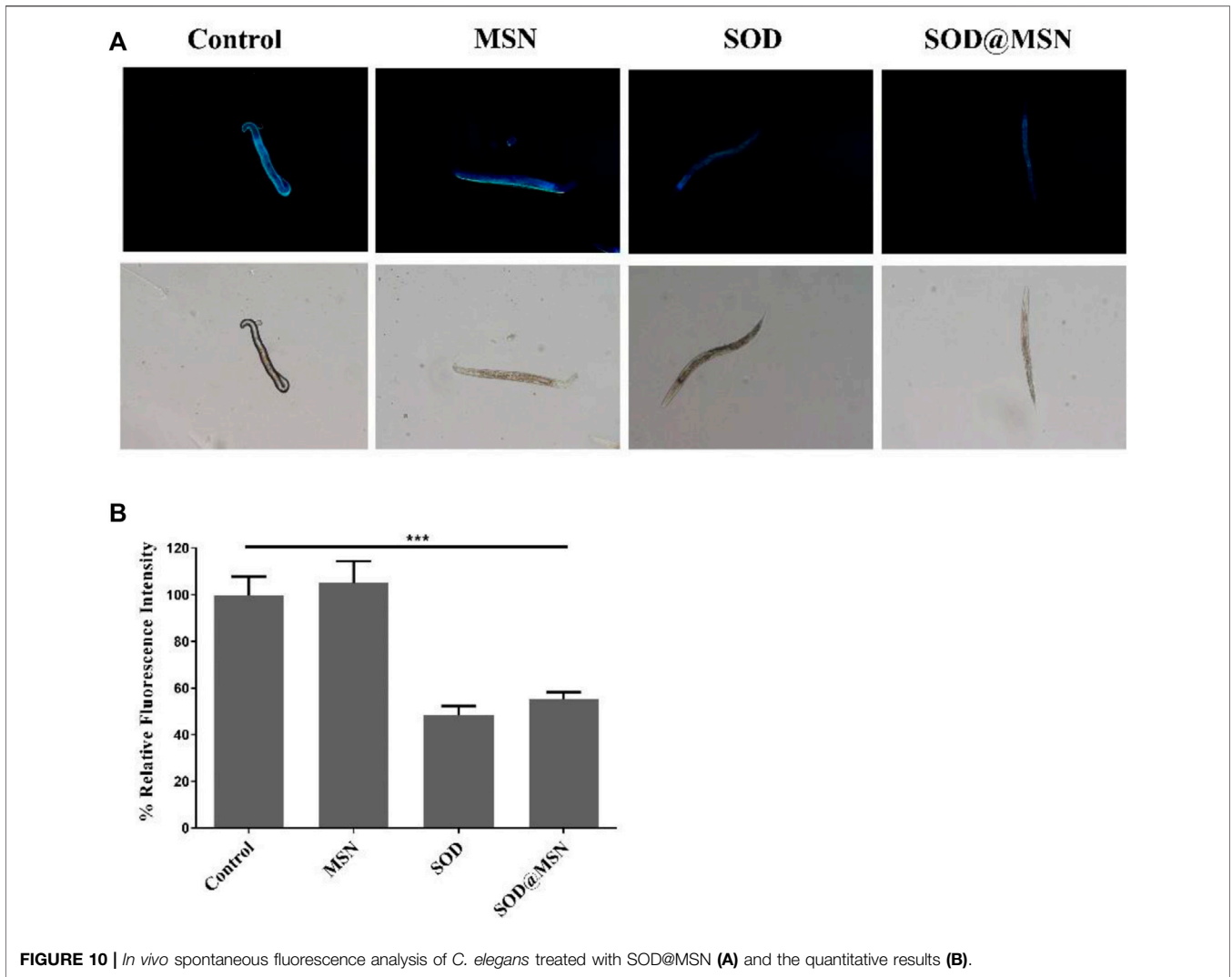


FIGURE 10 | *In vivo* spontaneous fluorescence analysis of *C. elegans* treated with SOD@MSN (A) and the quantitative results (B).

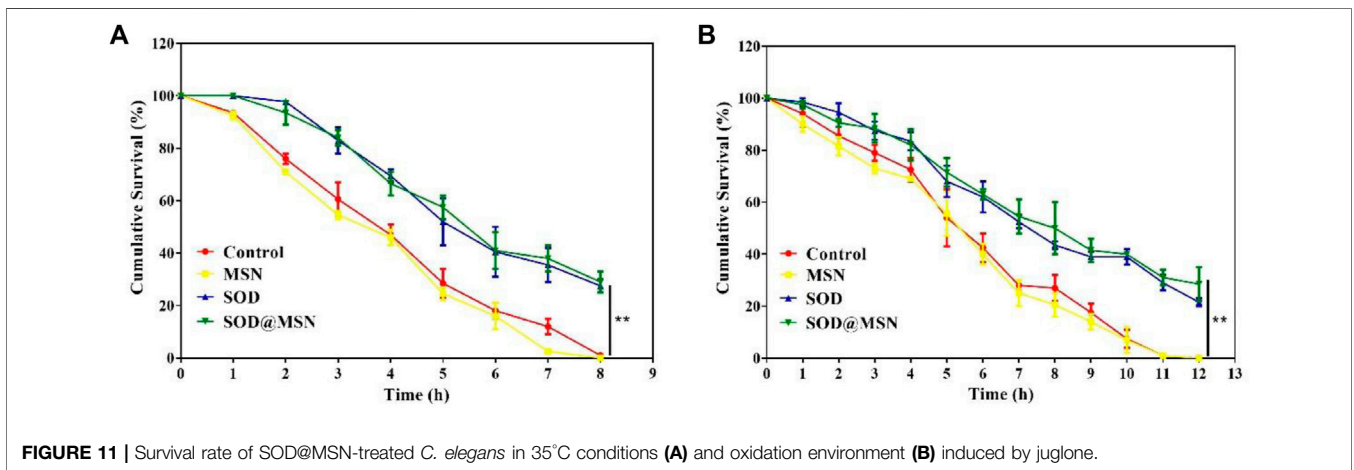


FIGURE 11 | Survival rate of SOD@MSN-treated *C. elegans* in 35°C conditions (A) and oxidation environment (B) induced by juglone.

SOD@MSN or free SOD treatment was also carried out, which suggested that the SOD activity attenuated more slowly after SOD@MSN treatment (Figure 7). The aforementioned

results indicated that SOD@MSN has better stability than free SOD in *C. elegans* and is expected to achieve a better therapeutic effect.

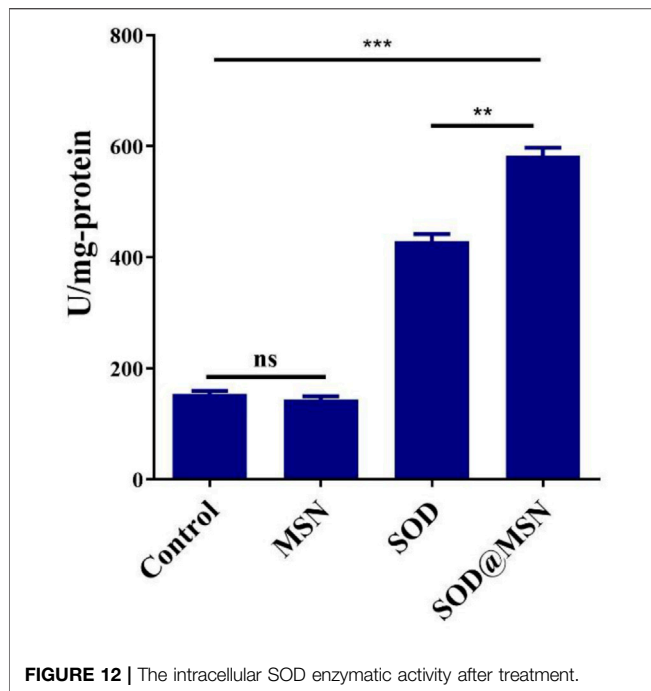


FIGURE 12 | The intracellular SOD enzymatic activity after treatment.

suggested that SOD@MSN and SOD had a satisfactory life-prolonging effect on wild-type *C. elegans*.

Effect of Superoxide Dismutase@ Mesoporous Silica Nanoparticles on the Healthspan of *C. elegans*

The longevity effect of SOD@MSN reminded us to study if it can improve the healthspan of *C. elegans*. First, Oil Red O was used to stain lipid deposits, which is a marker to reflect the body’s healthy levels of nematodes. As illustrated in Figure 9A, the fluorescence intensity in worms reduced significantly after treatment with SOD formulations compared with the control group. When quantified by ImageJ software, we found that the contents of lipid in N2 were reduced by 17.3% for SOD@MSN and 22% for SOD, respectively (Figure 9B). Furthermore, in contrast to the control group, the groups treated with SOD@MSN or free SOD released less blue fluorescence, as evidenced by the fluorescence microscope (Figure 10A). Quantification of the fluorescence revealed that about 48% and 55% of spontaneous fluorescence intensity was reduced in N2 with the treatment of drugs (Figure 10B). The aforementioned findings demonstrated that SOD@MSN could prominently improve the healthy levels of worms.

Effect of Superoxide Dismutase@ Mesoporous Silica Nanoparticles on the Lifespan of *C. elegans*

In order to determine the longevity effect of SOD@MSN on wild-type *C. elegans*, lifespan research was carried out, and 20°C was selected as the experimental temperature because it was optimal for *C. elegans*. As can be clearly illustrated in Figure 8 and Table 1, SOD@MSN and free SOD had the effect of prolonging the lifespan of worms with the mean lifespan increased from 10.23 to 16.12 and 14.04, respectively. In addition, the maximum lifespan of *C. elegans* also had a marked improvement with the treatment of SOD@MSN and free SOD. However, there was no effect after treating with MSN. The aforementioned results

Effect of Superoxide Dismutase@ Mesoporous Silica Nanoparticles on the Stress Tolerance of *C. elegans*

To determine if SOD@MSN could improve the stress tolerance ability of *C. elegans*, two different varieties of stress conditions were tested. First, thermo-tolerance ability of N2 was investigated using 35°C as thermal stimulation. The data suggested that SOD@MSN treatment significantly prolonged the survival time of N2 (Figure 11A). Similar results could also be found in the oxidative stress environment, in which juglone was used as the source of the oxidative stimulus. Juglone, as a kind of pro-oxidant, can produce superoxide anions in the presence of NAD(P)H and oxygen. Obviously, N2 animals treated with SOD@MSN or free SOD exhibited improved resistance against juglone, as can be proved

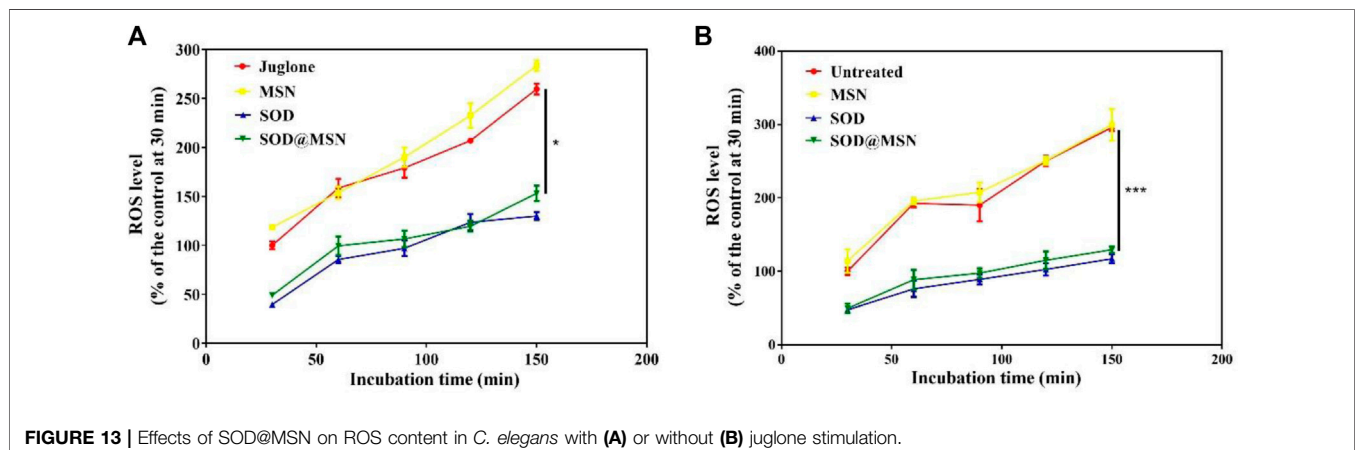
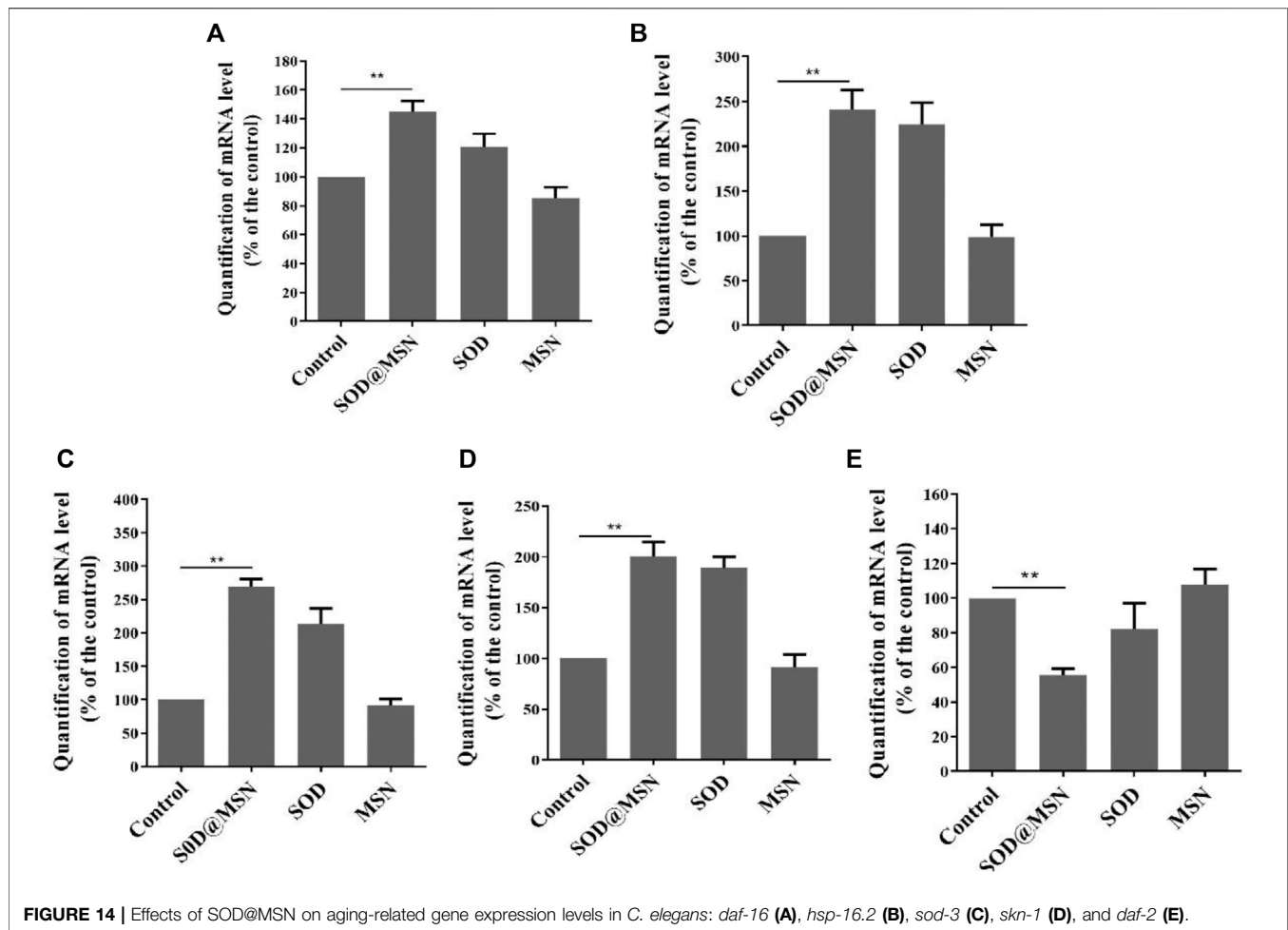


FIGURE 13 | Effects of SOD@MSN on ROS content in *C. elegans* with (A) or without (B) juglone stimulation.



by the increased survival rate after being pre-treated with SOD formulations (Figure 11B). The aforementioned results suggested that the worm's ability to resist heat and oxidative stress was elevated after pre-treatment with SOD@MSN, as can be evidenced by the increased survival numbers *C. elegans*.

Effect of Superoxide Dismutase@ Mesoporous Silica Nanoparticles on the Intracellular Superoxide Dismutase Enzymatic Activity and Reactive Oxygen Species Levels

To investigate the mechanism behind the effect of longevity and stress tolerance of *C. elegans* by SOD@MSN, the intracellular SOD enzymatic activity and ROS levels were detected. As obviously illustrated in Figure 12, the specific activity of SOD increased significantly after SOD@MSN treatment (compared with the control, $p < 0.001$; compared with the SOD group, $p < 0.01$). Furthermore, we found that the SOD activity was dramatically improved after SOD@MSN treatment than free SOD, which might be attributed to the longer staying time and higher enzyme activity in the case of the same dose of SOD.

Afterward, the ROS levels in *C. elegans* were determined under a regular culture medium, which revealed that SOD@MSN and free SOD obviously inhibited the production of intracellular ROS (Figure 13B, compared with the control, $p < 0.001$). Furthermore, juglone was used as an exogenous ROS irritant after treatment with SOD formulations. From Figure 13A we could find that the ROS levels in worms decreased significantly after being pre-treated with SOD@MSN or free SOD ($p < 0.05$), compared with the solvent-treated control N₂ *C. elegans*. The aforementioned results suggested that SOD@MSN prolonged the lifespan and strengthened the ability to resist the environmental stress by increasing the levels of antioxidant enzymes and reducing the ROS content in the body of *C. elegans*.

Effect of Superoxide Dismutase@ Mesoporous Silica Nanoparticles on the mRNA Expression of Genes Relevant to Aging and Stress Resistance

In order to investigate if the longevity and elevated stress tolerance of *C. elegans*. After SOD@MSN treatment was the result of the regulation of stress-response genes. Quantitative real-time PCR was therefore carried out to detect the expression

levels of genes, including *daf-2*, *daf-16*, *sod-3*, *skn-1*, and *hsp-16.2*. DAF-16 is responsible for both lifespan and stress response, and SOD-3 and HSP-16.2 are the downstream effectors of DAF-16. In addition, SKN-1 is another factor which plays a positive role in the regulation of lifespan and stress response. However, DAF-2 acts as an inhibitor of DAF-16 by phosphorylating DAF-16 and restricting its internalization into the cell nucleus. The results are shown in **Figure 14**, which reveal that SOD@MSN could significantly increase the expression of *daf-16* ($p < 0.01$), *sod-3* ($p < 0.01$), *hsp-16.2* ($p < 0.01$), and *skn-1* ($p < 0.05$) and reduce the expression of *daf-2* ($p < 0.01$). These results illustrated that the effect of SOD@MSN on the lifespan and stress tolerance was the result of regulation on the aging-related genes discussed earlier.

CONCLUSION

SOD was successfully immobilized on MSNs to develop an SOD@MSN nanoplatfom with desirable morphology and particle size. The research results suggested that SOD@MSN could be internalized by *C. elegans* effectively and kept stable for a longer time than with free SOD. In addition, SOD@MSN significantly prolonged the lifespan of *C. elegans* and extended the healthspan and lifespan during heat or/and oxidative stress. Further studies illustrated that the obvious longevity-extending effects of SOD@MSN on *C. elegans* were attributed to its free radical-scavenging capabilities. In addition, real-time PCR results demonstrated that the up-regulation of aging-associated genes, such as *daf-16*, *sod-3*, *hsp-16.2*, and *skn-1*, also contributed to the stress-resistance effect of SOD@MSN. These results indicated that the nanoplatfom could protect against environmental stress

REFERENCES

- Abedi Gaballu, F., Abbaspour-Ravasjani, S., Mansoori, B., Yekta, R., Hamishehkar, H., Mohammadi, A., et al. (2019). Comparative of *In-Vitro* Evaluation between Erlotinib Loaded Nanostructured Lipid Carriers and Liposomes against A549 Lung Cancer Cell Line. *Iran. J. Pharm. Res.* 18, 1168–1179. doi:10.22037/ijpr.2019.1100775
- Darroudi, S., Tajbakhsh, A., Esmaily, H., Ghazizadeh, H., Zamani, P., Sadabadi, F., et al. (2020). 50 Bp Deletion in Promoter Superoxide Dismutase 1 Gene and Increasing Risk of Cardiovascular Disease in Mashhad Stroke and Heart Atherosclerotic Disorder Cohort Study. *Biofactors* 46, 55–63. doi:10.1002/biof.1575
- Gao, F., Shao, T., Yu, Y., Xiong, Y., and Yang, L. (2021). Surface-bound Reactive Oxygen Species Generating Nanozymes for Selective Antibacterial Action. *Nat. Commun.* 12, 745. doi:10.1038/s41467-021-20965-3
- Huang, Y., Liu, Y., Shah, S., Kim, D., Simon-Soro, A., Ito, T., et al. (2021). Precision Targeting of Bacterial Pathogen via Bi-functional Nanozyme Activated by Biofilm Microenvironment. *Biomaterials* 268, 120581. doi:10.1016/j.biomaterials.2020.120581
- Koner, D., Banerjee, B., Kumari, A., Lanong, A. S., Snaitang, R., and Saha, N. (2021). Molecular Characterization of Superoxide Dismutase and Catalase Genes, and the Induction of Antioxidant Genes under the Zinc Oxide Nanoparticle-Induced Oxidative Stress in Air-Breathing Magur Catfish (*Clarias Magur*). *Fish. Physiol. Biochem.* 47 (6), 1909–1932. doi:10.1007/s10695-021-01019-3
- Li, Y., Tan, X., Liu, X., Liu, L., Fang, Y., Rao, R., et al. (2020). Enhanced Anticancer Effect of Doxorubicin by TPGS-Coated Liposomes with Bcl-2 siRNA-Corona for Dual Suppression of Drug Resistance. *Asian J. Pharm. Sci.* 15, 646–660. doi:10.1016/j.ajps.2019.10.003
- Liu, J., Xu, L., Shang, J., Hu, X., Yu, H., Wu, H., et al. (2021). Genome-wide Analysis of the Maize Superoxide Dismutase (SOD) Gene Family Reveals Important Roles in Drought and Salt Responses. *Genet. Mol. Biol.* 44, e20210035. doi:10.1590/1678-4685-GMB-2021-0035
- Liu, T., Xiao, B., Xiang, F., Tan, J., Chen, Z., Zhang, X., et al. (2020). Ultrasmall Copper-Based Nanoparticles for Reactive Oxygen Species Scavenging and Alleviation of Inflammation Related Diseases. *Nat. Commun.* 11, 2788. doi:10.1038/s41467-020-16544-7
- Liu, Y., Cheng, Y., Zhang, H., Zhou, M., Yu, Y., Lin, S., et al. (2020). Integrated Cascade Nanozyme Catalyzes *In Vivo* ROS Scavenging for Anti-inflammatory Therapy. *Sci. Adv.* 6, eabb2695. doi:10.1126/sciadv.abb2695
- Ma, M., Liu, Z., Gao, N., Pi, Z., Du, X., Ren, J., et al. (2020). Self-Protecting Biomimetic Nanozyme for Selective and Synergistic Clearance of Peripheral Amyloid- β in an Alzheimer's Disease Model. *J. Am. Chem. Soc.* 142, 21702–21711. doi:10.1021/jacs.0c08395
- Meyer, J. N., Lord, C. A., Yang, X. Y., Turner, E. A., Badireddy, A. R., Marinakos, S. M., et al. (2010). Intracellular Uptake and Associated Toxicity of Silver Nanoparticles in *Caenorhabditis elegans*. *Aquat. Toxicol.* 100, 140–150. doi:10.1016/j.aquatox.2010.07.016
- Owusu-Ansah, E., Song, W., and Perrimon, N. (2013). Muscle Mitohormesis Promotes Longevity via Systemic Repression of Insulin Signaling. *Cell* 155, 699–712. doi:10.1016/j.cell.2013.09.021
- Portegijs, E., Saajanaho, M., Leppä, H., Koivunen, K., Eronen, J., and Rantanen, T. (2022). Impact of Mobility Restrictions on Active Aging: Cross-Sectional Associations and Longitudinal Changes Parallel to COVID-19 Restrictions. *Arch. Gerontol. Geriatr.* 98, 104522. doi:10.1016/j.archger.2021.104522

and thus improve the healthspan and survival status, ultimately benefiting the lifespan of *C. elegans*.

DATA AVAILABILITY STATEMENT

The original contributions presented in the study are included in the article/**Supplementary Material**; further inquiries can be directed to the corresponding authors.

AUTHOR CONTRIBUTIONS

YY and JZ: manuscript preparation, figures and table preparation, and manuscript editing and revision. WW and KL: literature collection and evaluation, and draft manuscript preparation.

FUNDING

We greatly acknowledge the financial support from the National key R&D program of China (2017YFC0909900), Henan Province Medical Science and Technology Public Relations Plan Province Department joint construction project (LHGJ20200373).

SUPPLEMENTARY MATERIAL

The Supplementary Material for this article can be found online at: <https://www.frontiersin.org/articles/10.3389/fbioe.2022.795620/full#supplementary-material>

- Qi, S., Guo, L., Yan, S., Lee, R. J., Yu, S., and Chen, S. (2019). Hypocrellin A-Based Photodynamic Action Induces Apoptosis in A549 Cells through ROS-Mediated Mitochondrial Signaling Pathway. *Acta Pharm. Sin. B* 9, 279–293. doi:10.1016/j.apsb.2018.12.004
- Qin, T., Ma, S., Miao, X., Tang, Y., Huangfu, D., Wang, J., et al. (2020). Mucosal Vaccination for Influenza Protection Enhanced by Catalytic Immune-Adjuvant. *Adv. Sci.* 7, 2000771. doi:10.1002/advs.202000771
- Rao, Y. L., Ganaraja, B., Marathe, A., Manjrekar, P. A., Joy, T., Ullal, S., et al. (2021). Comparison of Malondialdehyde Levels and Superoxide Dismutase Activity in Resveratrol and Resveratrol/donepezil Combination Treatment Groups in Alzheimer's Disease Induced Rat Model. *Biotech.* 11, 329. doi:10.1007/s13205-021-02879-5
- Shi, S., Wu, S., Shen, Y., Zhang, S., Xiao, Y., He, X., et al. (2018). Iron Oxide Nanozyme Suppresses Intracellular Salmonella Enteritidis Growth and Alleviates Infection *In Vivo*. *Theranostics* 8, 6149–6162. doi:10.7150/thno.29303
- Singh, N., Savanur, M. A., Srivastava, S., D'Silva, P., and Muges, G. (2017). A Redox Modulatory Mn3 O4 Nanozyme with Multi-Enzyme Activity Provides Efficient Cytoprotection to Human Cells in a Parkinson's Disease Model. *Angew. Chem. Int. Ed.* 56, 14267–14271. doi:10.1002/anie.201708573
- Udipi, K., Ornberg, R. L., Thurmond, K. B., 2nd, Settle, S. L., Forster, D., and Riley, D. (2000). Modification of Inflammatory Response to Implanted Biomedical Materials *In Vivo* by Surface Bound Superoxide Dismutase Mimics. *J. Biomed. Mat. Res.* 51, 549–560. doi:10.1002/1097-4636(20000915)51:4<549::aid-jbm2>3.0.co;2-z
- von Baeckmann, C., Guillet-Nicolas, R., Renfer, D., Kählig, H., and Kleitz, F. (2018). A Toolbox for the Synthesis of Multifunctionalized Mesoporous Silica Nanoparticles for Biomedical Applications. *ACS Omega* 3, 17496–17510. doi:10.1021/acsomega.8b02784
- Wang, P., Chen, S., Cao, Z., and Wang, G. (2017). NIR Light-, Temperature-, pH-, and Redox-Responsive Polymer-Modified Reduced Graphene Oxide/mesoporous Silica Sandwich-like Nanocomposites for Controlled Release. *ACS Appl. Mat. Interfaces* 9, 29055–29062. doi:10.1021/acsami.7b07468
- Wang, T., Dong, H., Zhang, M., Wen, T., Meng, J., Liu, J., et al. (2020). Prussian Blue Nanoparticles Induce Myeloid Leukemia Cells to Differentiate into Red Blood Cells through Nanozyme Activities. *Nanoscale* 12, 23084–23091. doi:10.1039/d0nr06480g
- Wang, X., Li, C., Fan, N., Li, J., Zhang, H., Shang, L., et al. (2019). Amino Functionalized Chiral Mesoporous Silica Nanoparticles for Improved Loading and Release of Poorly Water-Soluble Drug. *Asian J. Pharm. Sci.* 14, 405–412. doi:10.1016/j.ajps.2018.04.002
- Wang, X., Tan, L.-L., Li, X., Song, N., Li, Z., Hu, J.-N., et al. (2016). Smart Mesoporous Silica Nanoparticles Gated by Pillararene-Modified Gold Nanoparticles for On-Demand Cargo Release. *Chem. Commun.* 52, 13775–13778. doi:10.1039/c6cc08241f
- Wang, Z., Dong, K., Liu, Z., Zhang, Y., Chen, Z., Sun, H., et al. (2017). Activation of Biologically Relevant Levels of Reactive Oxygen Species by Au/g-C3n4 Hybrid Nanozyme for Bacteria Killing and Wound Disinfection. *Biomaterials* 113, 145–157. doi:10.1016/j.biomaterials.2016.10.041
- Wen, J., Yang, K., Liu, F., Li, H., Xu, Y., and Sun, S. (2017). Diverse Gatekeepers for Mesoporous Silica Nanoparticle Based Drug Delivery Systems. *Chem. Soc. Rev.* 46, 6024–6045. doi:10.1039/c7cs00219j
- Wu, Z., Liu, Q., Zhang, Y., Guan, X., Xiu, M., and Zhang, X. (2021). Superoxide Dismutase, BDNF and Cognitive Improvement in Drug-Naive First Episode Patients with Schizophrenia: a 12-week Longitudinal Study. *Int. J. Neuropsychopharmacol.* 25 (2), 128–135. doi:10.1093/ijnp/pyab065
- Wurm, S., Wiest, M., Wolff, J. K., Beyer, A.-K., and Spuling, S. M. (2020). Changes in Views on Aging in Later Adulthood: The Role of Cardiovascular Events. *Eur. J. Ageing* 17, 457–467. doi:10.1007/s10433-019-00547-5
- Xi, J., Zhang, R., Wang, L., Xu, W., Liang, Q., Li, J., et al. (2020). A Nanozyme-Based Artificial Peroxisome Ameliorates Hyperuricemia and Ischemic Stroke. *Adv. Funct. Mater.* 31, 2007130. doi:10.1002/adfm.202007130
- Xia, X.-F., Zheng, J.-J., Shao, G.-M., Wang, J.-L., Liu, X.-S., and Wang, Y.-F. (2013). Cloning and Functional Analysis of Glutathione Peroxidase Gene in Red Swamp Crayfish *Procambarus clarkii*. *Fish Shellfish Immunol.* 34, 1587–1595. doi:10.1016/j.fsi.2013.03.375
- Xu, L., Liang, Y., Xu, X., Xia, J., Wen, C., Zhang, P., et al. (2021). Blood Cell-Derived Extracellular Vesicles: Diagnostic Biomarkers and Smart Delivery Systems. *Bioengineered* 12, 7929–7940. doi:10.1080/21655979.2021.1982320
- Yang, B., Chen, Y., and Shi, J. (2019). Reactive Oxygen Species (ROS)-based Nanomedicine. *Chem. Rev.* 119, 4881–4985. doi:10.1021/acs.chemrev.8b00626
- Yee, C., Yang, W., and Hekimi, S. (2014). The Intrinsic Apoptosis Pathway Mediates the Pro-longevity Response to Mitochondrial ROS in *C. elegans*. *Cell* 157, 897–909. doi:10.1016/j.cell.2014.02.055
- Yu, D., Ma, M., Liu, Z., Pi, Z., Du, X., Ren, J., et al. (2020). MOF-encapsulated Nanozyme Enhanced siRNA Combo: Control Neural Stem Cell Differentiation and Ameliorate Cognitive Impairments in Alzheimer's Disease Model. *Biomaterials* 255, 120160. doi:10.1016/j.biomaterials.2020.120160
- Zhang, L., Bei, H. P., Piao, Y., Wang, Y., Yang, M., and Zhao, X. (2018). Polymer-brush-grafted Mesoporous Silica Nanoparticles for Triggered Drug Delivery. *Chemphyschem* 19, 1956–1964. doi:10.1002/cphc.201800018
- Zhang, S., Liu, Y., Sun, S., Wang, J., Li, Q., Yan, R., et al. (2021). Catalytic Patch with Redox Cr/CeO2 Nanozyme of Noninvasive Intervention for Brain Trauma. *Theranostics* 11, 2806–2821. doi:10.7150/thno.51912
- Zhang, Z., Zhao, Y., Wang, X., Lin, R., Zhang, Y., Ma, H., et al. (2016). The Novel Dipeptide Tyr-Ala (TA) Significantly Enhances the Lifespan and Healthspan of *Caenorhabditis elegans*. *Food Funct.* 7, 1975–1984. doi:10.1039/c5fo01302j
- Zhao, J., Gao, W., Cai, X., Xu, J., Zou, D., Li, Z., et al. (2019). Nanozyme-mediated Catalytic Nanotherapy for Inflammatory Bowel Disease. *Theranostics* 9, 2843–2855. doi:10.7150/thno.33727

Conflict of Interest: The authors declare that the research was conducted in the absence of any commercial or financial relationships that could be construed as a potential conflict of interest.

Publisher's Note: All claims expressed in this article are solely those of the authors and do not necessarily represent those of their affiliated organizations, or those of the publisher, the editors, and the reviewers. Any product that may be evaluated in this article, or claim that may be made by its manufacturer, is not guaranteed or endorsed by the publisher.

Copyright © 2022 Yang, Wang, Liu and Zhao. This is an open-access article distributed under the terms of the Creative Commons Attribution License (CC BY). The use, distribution or reproduction in other forums is permitted, provided the original author(s) and the copyright owner(s) are credited and that the original publication in this journal is cited, in accordance with accepted academic practice. No use, distribution or reproduction is permitted which does not comply with these terms.